



Supplement of

HUB: a method to model and extract the distribution of ice nucleation temperatures from drop-freezing experiments

Ingrid de Almeida Ribeiro et al.

Correspondence to: Valeria Molinero (valeria.molinero@utah.edu)

The copyright of individual parts of the supplement might differ from the article licence.

S1 Effect of the number of droplets and dilutions on the temperature range of the cumulative freezing spectrum $N_m(T)$

5 Table S1: Mean relative error (MRE) and parameters of the differential freezing spectrum $n_m(T)$ obtained using the HUB-backward code. The data was generated with the HUB-forward code using the following parameters to set the underlying distribution of heterogeneous freezing temperatures: $T_{mode,1}=-8$ °C, $T_{mode,2}=-4$ °C, $s_1 = s_2 = 0.5$, $c_1 = 0.9$ and $c_2 = 0.1$. To generate the data shown in Figure 6, 100 droplets were used to sample each concentration and we used a bin width of 0.1.

Concentrations	MRE	$T_{mode,1}(^{\circ}\text{C})$	s_1	$T_{mode,2}(^{\circ}\text{C})$	s_2	c_2	β
$10^4, 10^3, 10^2, 10^1, 10^0$	13%	-7.9	0.55	-3.9	0.50	0.16	0.63
$10^4, 10^3, 10^2, 10^1$	76%	-7.3	0.11	-4.1	0.52	0.43	0.56
$10^3, 10^2, 10^1, 10^0$	13%	-7.9	0.56	-4.0	0.50	0.16	0.63
$10^2, 10^1, 10^0$	14%	-7.9	0.54	-4.0	0.52	0.16	0.63

10 Table S2: Mean relative error (MRE) and parameters of the differential freezing spectrum obtained using the HUB-backward code. The data was generated with the HUB-forward code using the following parameters to set the underlying distribution of heterogeneous freezing temperatures: $T_{mode,1}=-8$ °C, $T_{mode,2}=-4$ °C, $s_1 = s_2 = 0.5$, $c_1 = 0.999$ and $c_2 = 0.001$. To generate the data shown in Figure 7, 100 droplets were used to sample each concentration and we used a bin width of 0.1.

Concentrations	MRE	$T_{mode,1}(^{\circ}\text{C})$	s_1	$T_{mode,2}(^{\circ}\text{C})$	s_2	c_2	β
$10^4, 10^3, 10^2, 10^1, 10^0$	6%	-7.8	0.45	-4.0	0.54	1.2×10^{-3}	0.63
$10^4, 10^3, 10^2, 10^1$	130%	-7.0	0.17	-4.0	0.52	7.9×10^{-3}	0.23
$10^3, 10^2, 10^1, 10^0$	7%	-7.8	0.46	-3.7	0.32	1.0×10^{-3}	0.64
$10^2, 10^1, 10^0$	94%	-7.8	0.46	-3.9	0.80	1.0×10^{-3}	0.55

15 Table S3: Mean relative error (MRE) and parameters of the differential freezing spectrum obtained using the HUB-backward code. The data was generated with the HUB-forward code using the following parameters to set the underlying distribution of heterogeneous freezing temperatures: $T_{mode,1}=-8$ °C, $T_{mode,2}=-4$ °C, $s_1 = s_2 = 0.5$, $c_1 = 0.999$ and $c_2 = 0.001$. To generate the data shown in Figure 8, 25 droplets were used to sample each concentration and we used a bin width of 0.1.

Concentrations	MRE	$T_{mode,1}(^{\circ}\text{C})$	s_1	$T_{mode,2}(^{\circ}\text{C})$	s_2	c_2	β
$10^4, 10^3, 10^2, 10^1, 10^0$	38%	-8.0	0.52	-4.3	0.61	3.0×10^{-3}	0.62
$10^3, 10^2, 10^1, 10^0$	36%	-7.9	0.50	-4.1	0.57	3.0×10^{-3}	0.62
$10^2, 10^1, 10^0$	7600%	-8.4	0.24	-7.6	0.38	0.455	0.63

S2 Obtaining the differential freezing spectrum $n_m(T)$ from the experimental cumulative freezing spectrum $N_m(T)$ of biological INs using the HUB-backward code

20

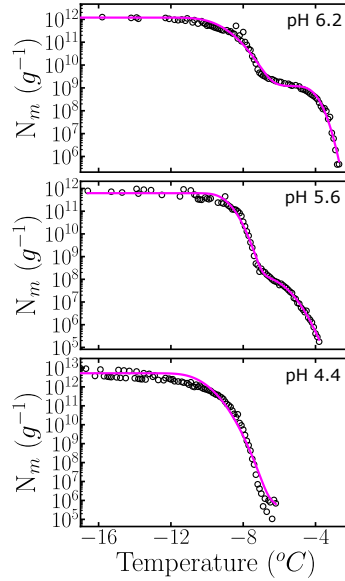


Figure S1: Cumulative freezing spectra $N_m(T)$ obtained from drop-freezing experiments for *P. Syringae* (Lukas et al., 2020) black circles). The magenta lines represent $N_m(T)$ calculated with the optimized solution $n_m^{optimized}(T)$ composed of a combination of two Gaussian distributions.

25

Table S4: Mean relative error (MRE) and parameters of the differential freezing spectrum obtained using the HUB-backward code.

pH	MSE	$T_{mode,1}(^{\circ}C)$	s_1	$T_{mode,2}(^{\circ}C)$	s_2	c_2	β
6.2	0.02	-9.3	0.93	-4.1	0.43	1.3×10^{-3}	0.43
5.6	0.02	-8.7	0.54	-6.4	0.86	5.0×10^{-4}	0.48
4.4	0.04	-10.4	0.77	-6.3	0.87	3.3×10^{-7}	0.34

S3 Obtaining the differential freezing spectrum $n_m(T)$ from the experimental fraction of ice $f_{ice}(T)$ of insoluble ice nucleants using the HUB-backward code

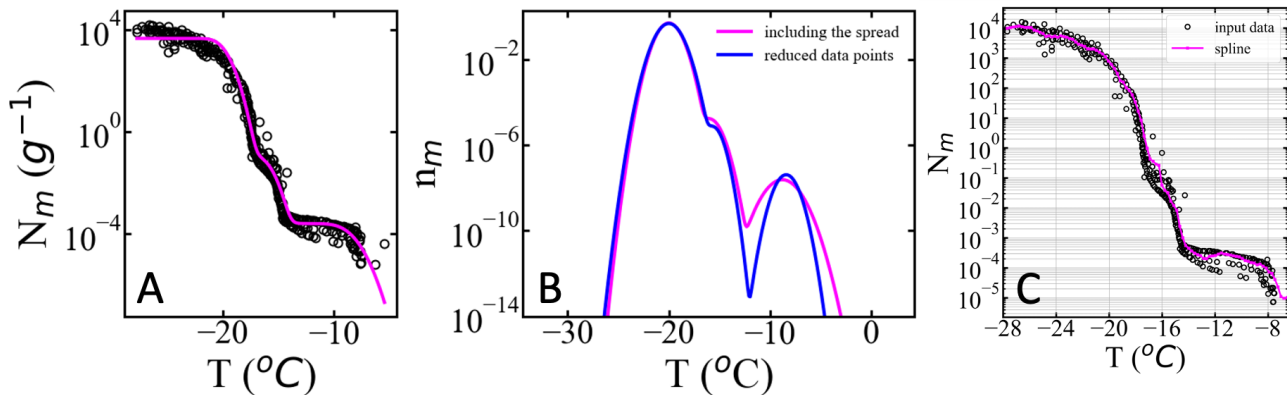
30

Table S5: Mean relative error (MRE) and parameters of the differential freezing spectrum obtained using the HUB-backward code from the cholesterol data with two different cooling rates (Zhang and Maeda, 2022).

	MSE	$T_{mode,1}(^{\circ}C)$	s_1	$T_{mode,2}(^{\circ}C)$	s_2	c_2	$T_{mode,3}(^{\circ}C)$	s_3	c_3
0.18K/min	2×10^{-4}	-15.6	1.00	-10.7	1	0.41	-7.2	1.00	0.43
0.06K/min	2×10^{-4}	-13.6	0.80	-9.0	0.86	0.29	-6.5	0.80	0.54

S4 Effect of sparse sampling of a cumulative spectrum on the estimation of the differential spectrum with HUB-backward

35 **Figure 9E-F** presents an analysis of a sample of the pollen data of (Dreischmeier, 2019). **Supp. Fig. S2** shows that the analysis of the full data set shown **Fig. 9E** produces an almost identical differential spectrum, because HUB-backward interpolates the input data to produce a smooth and equally spaced data set (**Supp. Fig. S3**).



40 **Figure S2: Effect of sparsely sampling a dense data set. A)** cumulative spectra (black circles) of pollen from (Dreischmeier, 2019) and its fitting to two populations with HUB-backward fitting (magenta line). **B)** differential spectrum derived by that analysis from the analysis of all experimental data points (magenta line) is almost indistinguishable from the one obtained by sparsely sampling the data set (blue line, also shown in Fig 9F). **C)** cumulative spectra (black circles) of pollen from (Dreischmeier, 2019) used as input for HUB-backward and interpolated data using the default parameters of the code (magenta line).

45 S5 Modeling the differential spectrum of systems with chemical or phase equilibria using the HUB-backward code

In the derivation of the HUB method, we have assumed that the average number λ of IN per droplet is proportional to the dilution of the sample. The IN, however, can be involved in chemical or phase equilibria that would impact the proportionality between λ and dilution. The result is a mismatch between the actual concentration of IN in solution and the total mass concentration of the sample. Ice nucleation of Lignin provides such an example (Bogler and Borduas-Dedekind, 2020). This data set combines two challenges. First, that the nucleation from the background water used to prepare the samples produces fraction of ice signal that is highly overlapped with that of the samples themselves (**Fig. S2-A**). This is a characteristic shared by all poor ice nucleants. Second, that the processing of the fraction of ice curves using Vali's equation (**Eq. 1.a** of the manuscript) result in cumulative spectra that do not overlap (**Fig. S2-B**). This implies that the concentration

50

of IN is not proportional to the dilution (in this case, given by the total mass of organic carbon in the sample). In this example, the $N_m(T)$ curves seem to be parallel, suggesting that the nature of the IN is preserved across concentrations, but there is an aggregation equilibrium that makes its concentration increase in a sublinear manner with sample concentration. **Fig. S2-C** shows the differential spectrum n_m obtained with HUB-backward from the fraction of frozen droplets of each concentration; these fits are shown with colored lines in **Fig. S2-A** and faithfully represent each of the $f_{ice}(T)$ curves. As expected from extreme value statistics with incomplete sampling, the $n_m(T)$ depends on the concentration (see also **Fig 2C** of the main text). The way the peaks move seems to be consistent with the analysis of extreme value statistics, but it is necessary to remove the background in order to do a better analysis.

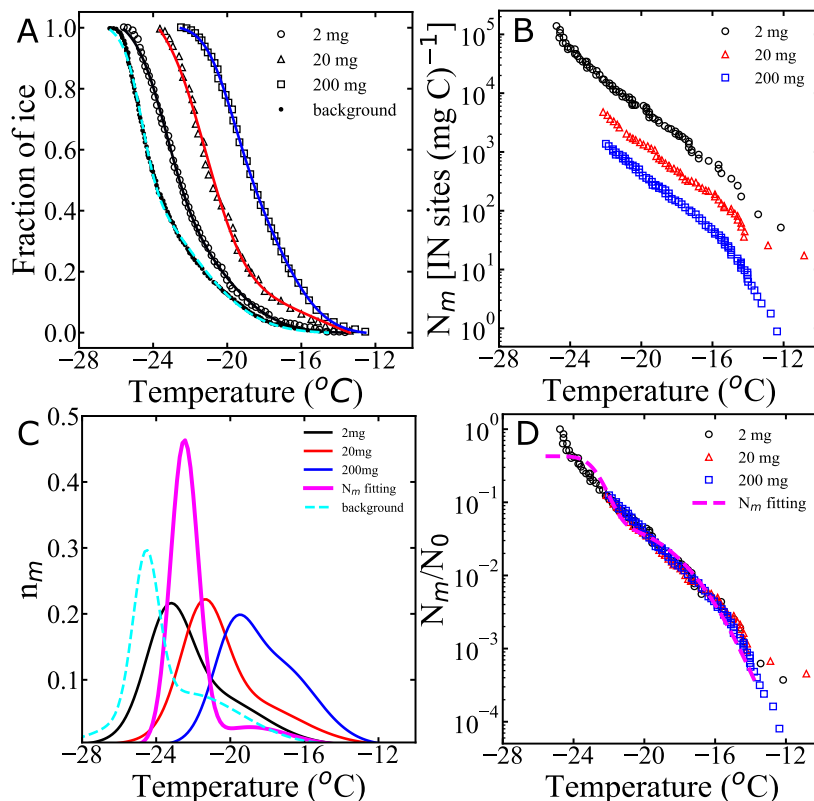
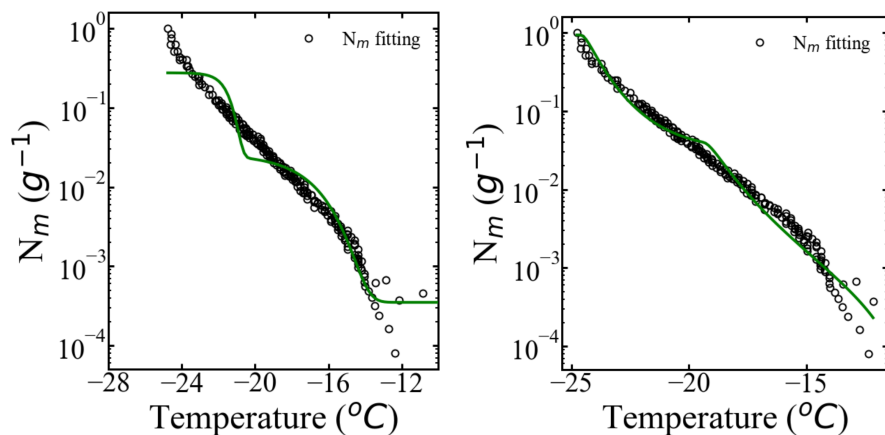


Figure S3: A) Fraction of ice for different concentrations of Lignin (Bogler and Borduas-Dedekind, 2020). Continuous lines represent the fitting of the fraction of frozen droplets obtained with the HUB-backward code using two subpopulations and Gaussian distributions as working basis. B) Cumulative freezing spectrum N_m obtained from Ref. (Bogler and Borduas-Dedekind, 2020). C) The differential freezing spectrum n_m obtained from the fitting shown by continuous lines in A). D) Points represent scaled cumulative freezing spectrum, and magenta dashed line is the fitting of the cumulative spectrum using HUB-backward.



70

Figure S4: Fitting of N_m using HUB-backward with two subpopulations with a left-tail Gumbel (left), and log-normal (right).

Table S6: Mean relative error (MRE) and parameters of the differential freezing spectrum obtained using the HUB-backward code from lignin data at various concentrations (Bogler and Borduas-Dedekind, 2020).

	MSE	$T_{mode,1}(^{\circ}\text{C})$	s_1	$T_{mode,2}(^{\circ}\text{C})$	s_2	c_2
2 mg	2×10^{-4}	-21.05	2.68	-23.33	1.20	0.49
20 mg	2×10^{-4}	-21.46	1.20	-19.24	2.85	0.48
200 mg	2×10^{-4}	-19.84	1.11	-17.51	2.09	0.65
background	2×10^{-4}	-24.55	0.70	-22.40	2.95	0.59
N_m fitting (Gaussian)	0.010	-22.48	0.74	-18.93	2.10	0.14
N_m fitting (log-normal)	0.015	-24.64	0.79	-19.42	0.77	0.05

75 References

Bogler, S. and Borduas-Dedekind, N.: Lignin's ability to nucleate ice via immersion freezing and its stability towards physicochemical treatments and atmospheric processing, *Atmos. Chem. Phys.*, 20, 14509-14522, 10.5194/acp-20-14509-2020, 2020.

Dreischmeier, K.: Heterogene Eisnukleations- und Antifrefriereigenschaften von Biomolekülen, Bielefeld University, <https://doi.org/10.4119/unibi/2907691>, 2019.

80 Lukas, M., Schwidetzky, R., Kunert, A. T., Pöschl, U., Fröhlich-Nowoisky, J., Bonn, M., and Meister, K.: Electrostatic Interactions Control the Functionality of Bacterial Ice Nucleators, *Journal of the American Chemical Society*, 142, 6842-6846, 10.1021/jacs.9b13069, 2020.

Zhang, X. and Maeda, N.: Nucleation curves of ice in the presence of nucleation promoters, *Chemical Engineering Science*, 262, 118017, <https://doi.org/10.1016/j.ces.2022.118017>, 2022.

85